

Generation of a rhesus macaque harboring a multivalent reporter for assessing gene editing outcomes

Received: 19 January 2026

Accepted: 4 May 2026

Published online: 19 May 2026

Cite this article as: Ryu J., Ryder K., Naka H. *et al.* Generation of a rhesus macaque harboring a multivalent reporter for assessing gene editing outcomes. *Sci Rep* (2026). <https://doi.org/10.1038/s41598-026-52214-2>

Junghyun Ryu, Kristie Ryder, Hiroaki Naka, Jenni Tran, Brayden J. Hinrichs, Sreya Biswas, Lauren N. Rust, Sofiya Yusova, Brandy L. Dozier, Samuel M. Peterson, Jochen M. Wettengel, Carol B. Hanna, Jon D. Hennebold, Benjamin J. Burwitz & Benjamin N. Bimber

We are providing an unedited version of this manuscript to give early access to its findings. Before final publication, the manuscript will undergo further editing. Please note there may be errors present which affect the content, and all legal disclaimers apply.

If this paper is publishing under a Transparent Peer Review model then Peer Review reports will publish with the final article.

Generation of a Rhesus Macaque Harboring a Multivalent Reporter for Assessing Gene Editing**Outcomes**

Junghyun Ryu ¹, Kristie Ryder ², Hiroaki Naka ², Jenni Tran ⁴, Brayden J. Hinrichs ⁴, Sreya Biswas ⁴, Lauren N. Rust ⁴, Sofiya Yusova ⁴, Brandy L. Dozier ⁵, Samuel M. Peterson ², Jochen M. Wettengel ^{6,7}, Carol B. Hanna ¹, Jon D. Hennebold ^{1,8}, Benjamin J. Burwitz ^{3,4}, Benjamin N. Bimber ^{2,3,*}

* Corresponding author. Email: bimber@ohsu.edu, Phone: 503-418-2755

¹ Division of Reproductive & Developmental Sciences, Oregon National Primate Research Center, Oregon Health & Science University, Beaverton, OR 97006, USA

² Division of Genetics, Oregon National Primate Research Center, Oregon Health & Science University, Beaverton, OR, 97006, USA.

³ Vaccine & Gene Therapy Institute, Oregon Health & Science University, Beaverton, OR 97006, USA.

⁴ Division of Pathobiology & Immunology, Oregon National Primate Research Center, Oregon Health & Science University, Beaverton, OR 97006, USA.

⁵ Division of Comparative Medicine, Oregon National Primate Research Center, Oregon Health & Science University, Beaverton, OR 97006, USA.

⁶ Institute of Virology, School of Medicine and Health, Technical University of Munich/Helmholtz Munich, Munich, Germany.

⁷ German Center for Infection Research (DZIF), Munich partner site, Munich, Germany.

⁸ Department of Obstetrics & Gynecology, Oregon Health & Science University, Portland, OR 97239, USA.

ABSTRACT

Somatic gene editing therapies offer the potential for lasting treatments for a range of genetic disorders, with a host of therapies at various stages of clinical testing. The development of safe, effective therapies required relevant pre-clinical animal models capable of measuring on-target delivery and detecting off-target editing. Here we present the creation of a transgenic rhesus macaque encoding the Bivalent Enhanced Traffic Light Editing (BETLE) system, a multi-color fluorescent reporter that provides a simple readout for multiple modes of gene editing, including off-target effects. We used zygote microinjection and piggyBac transposase to generate preimplantation embryos that ultimately led to a healthy transgenic macaque. Extensive molecular analyses demonstrated single-copy integration of the intact reporter; however, the animal was mosaic, with only 5-8% of cells encoding the reporter, although all germ layers contained positive cells. The creation of this macaque provides important information to improve future transgenics, and progeny from this macaque could provide a powerful tool to evaluate the delivery and accuracy of gene therapies.

ARTICLE IN PRESS

INTRODUCTION

Genetically altered animal models are extremely powerful systems that have yielded invaluable insight into human disease and advanced our understanding of foundational biological processes. Rodents are the most common platform for genetic manipulation; however, there are many human diseases and processes that can only be effectively modeled in closely related primate species^{1,2}. Rhesus macaques (RMs), which share similar anatomy and physiology of various organ systems with humans, are highly valued models for studies in neuroscience, reproduction, and infectious disease^{1,3-14}. Additionally, the high degree of genetic sequence similarity between humans and rhesus macaques may provide more informative insights into off-target events following somatic gene therapy testing.

Despite advances in gene editing technologies, it remains extremely challenging to generate genetically altered non-human primates, as outlined in several recent reviews¹⁵⁻¹⁸. As a result, despite the birth of the first transgenic RM in 2001, there have been relatively few genetically altered macaques born in the subsequent two decades¹⁵. The vast majority of published transgenic rhesus and cynomolgus macaques were generated by microinjection of editing material into oocytes near the time of fertilization or zygotes, followed by embryo implantation into a surrogate female¹⁹⁻²¹. Unlike rodents, the production of oocytes in RMs is a rate-limiting step in the generation of genetically altered animals.

Multiple modes of germline editing have been demonstrated in RMs, and each has pros and cons for different research goals. The earliest examples of germline editing in RMs used randomly integrating lentiviruses to deliver an exogenous gene, such as GFP or a defective copy of the *MCPH1* gene^{22,23}. CRISPR/Cas9 technologies have been utilized, although the most common usage of these to date is disruption of an endogenous gene, not the delivery of exogenous DNA^{19,24}. The use of CRISPR/Cas9 and homology-directed repair (HDR) has been reported for germline editing of a short, localized region, such as the introduction of ~200 bp of CAG repeats into the huntingtin gene²⁵. In addition to rhesus macaque germline editing, there are many published examples of germline edited cynomolgus macaques, which utilize the same set of technologies and face similar challenges¹⁵. Knock-in of exogenous genetic material represents an important category of genetic modifications, such as the introduction of an inducible reporter molecule or

expression of a specific form of a gene (e.g., the human form of a protein or a defective, disease-inducing variant). While CRISPR/Cas9 and HDR can in theory be used to deliver large exogenous DNA, efficiency decreases considerably with the size of the insert, rendering it problematic for non-human primates²⁶. Lentiviral vectors suffer from limitations in cargo size, and the inability to control copy number or site(s) of integration^{27,28}. The piggyBac system, which uses Tn5 transposase to randomly integrate cargo into the genome, has been recently used to create transgenic rhesus macaques encoding the human form of the NTCP receptor under the control of a liver-specific reporter or a multicolor reporter cassette^{29,30}.

In this study, we used zygote microinjection and the piggyBac transposase system to generate a healthy transgenic RM encoding an exogenous 5.5 kb reporter cassette, based on the Bivalent Enhanced Traffic Light Editing (BETLE) system³¹. BETLE is designed to provide fluorescent readouts for on- and off-target gene editing. RMs encoding BETLE provide an experimental platform to validate the delivery and off-target effects of human gene therapies. After birth, extensive molecular characterization revealed that while all germ layers encode BETLE, there is both mosaicism and negative epigenetic regulation of transgene expression *in vivo*. Due to these issues, the progenitor RM is unlikely to be suitable as an *in vivo* reporter; however, the techniques and extensive molecular characterization provide important information to guide the development of future transgenic RMs.

RESULTS

Creation of a transgenic rhesus macaque using piggyBac transposase:

Expression of an exogenous construct is an important category of germline editing and is a critical step for the creation of many categories of genetic models. The most common modes of transgene delivery used in macaques are randomly integrating vectors, such as lentiviruses. Tn5 transposase systems, such as Sleeping Beauty or piggyBac, are alternatives that also randomly integrate, but can be used to deliver much larger cargo³²⁻³⁴. Our study had two primary objectives. First, we sought to demonstrate the feasibility of germline delivery of a large exogenous construct to a non-human primate genome using piggyBac transposase. We selected the Bivalent Enhanced Traffic Light Editing (BETLE) system as proof-of-concept. BETLE is a multifunctional reporter platform capable of concurrently detecting gene disruption, frameshift mutations, and HDR through

dual fluorescent and luminescent readouts (**Fig. 1A**)³¹. The BETLE construct constitutively expresses the red fluorescent protein mCherry, under the control of the CAG promoter. Downstream of mCherry, it encodes a defective moxGFP (containing a 39 bp deletion), followed by a stop codon in the first reading frame. This is followed by mTagBFP2 in the +1/-2 reading frame, and NanoLuc in the +2/-1 reading frame. Genomic editing of BETLE that alters the downstream reading frame can induce expression of either reporter. As such, RMs encoding BETLE will provide a highly informative platform for the testing and validation of somatic gene editing reagents.

We used microinjection of zygotes to deliver the BETLE construct and piggyBac transposase. A total of 17 rounds of controlled ovarian stimulation (COS) were performed, yielding 418 oocytes from 14 female RMs. Of these, 264 were metaphase II (MII) oocytes, 63 were metaphase I (MI), 51 were germinal vesicle (GV) oocytes, and 40 were degenerated. For *in vitro* fertilization, all oocytes, excluding the degenerated, were used, resulting in 243 presumptive zygotes. All zygotes were injected into the pronucleus and cytoplasm with a plasmid encoding the BETLE construct flanked by terminal repeats (TRs), along with piggyBac mRNA. The piggyBac transposase mediates recombination between these TR sequences and genomic DNA (TTAA sites) to result in stable transgene integration. The injected embryos were cultured for 7-9 days, after which blastocysts were collected for trophectoderm (TE) biopsy. A total of 37 blastocysts were obtained, and TE biopsy samples were successfully collected from all of them. Genomic DNA from the TE biopsies was collected, whole genome amplification (WGA) performed, and then analyzed for BETLE integration using enhanced tagmentation-assisted PCR (esTag-PCR)³⁵. This assay uses primers specific to either end of the transgene to amplify transgene-genome junctions, thereby providing unbiased genome-wide detection and mapping of transgene integration sites with base-pair resolution. These results indicated that 12 out of 37 blastocysts carried the BETLE cassette, with an integration efficiency of 32.4% (**Fig. 1B**). As expected from a randomly integrating system, the copy number was highly variable per embryo (including arrested embryos), with an average of 2.8 integrations per embryo or 5.6 when excluding non-edited embryos (**Fig. 1C** and **Table S1**). Depending on blastocyst quality, 1-3 blastocysts were transferred into each surrogate animal. One of these embryo transfers, involving a single blastocyst, resulted in a successful pregnancy.

Birth of a transgenic RM and genomic characterization:

A 410 g healthy male infant was born (**Fig. 2A**) and successfully reared to weaning at 1 yr 12 d, exhibiting a normal growth trend (2.6 kg at 1 yr 22 d) during this time. The infant was named Fred (Fluorescent Red) due to the constitutive expression of the mCherry protein by the BETLE reporter. To verify the presence of BETLE across tissues, we collected tissues spanning multiple germ layers, including a buccal swab, as well as skin, liver, and rectal biopsies. We isolated genomic DNA and performed an identical esTag-PCR assay as previously performed on the TE material. Interestingly, while the TE biopsy predicted two integration sites, one on chromosome 5 and one on chromosome 12 (**Fig. 2B**), only one of these sites was detected in the tissues sampled after birth. All tissues contained an identical integration pattern, predicting a single integration site on chromosome 5, position 47,727,101 (based on the MMul_10 assembly). This discrepancy highlights a challenge with the reliance on TE biopsies: genetic discrepancies between trophectoderm and the remaining embryo can occur^{36,37}. With current technology there is no practical substitute, although this highlights the importance of additional genetic testing.

Next, we performed a panel of genomic assays to further verify the integrity of and location of the BETLE cassette. Using genomic DNA isolated from blood, we performed PCR amplification of the region encoding the BETLE cassette using overlapping PCR amplicons that span the cassette and include flanking genomic DNA (**Fig. 2C**). These amplicons were pooled, prepared for Illumina sequencing using the Nextera tagmentation system, and sequenced to high-depth (average coverage of 246.8) using Illumina short read chemistry. The resulting reads were aligned to the BETLE reference, demonstrating that the integrated cassette sequence matches the expected sequence (confirmed by manual inspection of the alignment and the LoFreq variant caller³⁸). These targeted sequence data are concordant with the esTag-PCR assay and confirm single-copy integration into chromosome 5 at position 47,727,101. To rule out the possibility of alternate integration events, we performed unbiased genome-wide long-read sequencing using PacBio chemistry, also using gDNA isolated from blood. The long-read data confirmed the intact integration of a single copy of the BETLE cassette into chromosome 5 and did not detect evidence for any additional copies of BETLE in the genome. Collectively, these three methods strongly support single copy integration of BETLE into chromosome 5, position 47,727,101, with concordant results across tissues derived from all three germ layers. Genome editing carries the potential of off-target effects, ranging from spurious integration events to small and large-scale chromosomal rearrangements. To evaluate potential off-target effects, the genome-wide

long-read data were aligned to the MMul_10 rhesus macaque reference genome, followed by both short and structural variant detection. No abnormal or large structural rearrangements were detected.

Mosaicism and weak mCherry RNA expression in vivo:

The BETLE cassette is a complex reporter that constitutively expresses the fluorescent protein mCherry (**Fig. 1A**). To validate expression of mCherry protein, we performed biopsies on liver, skin, and rectal tissue, followed by immunohistochemistry (**Fig. 3A**). We were unable to directly detect mCherry fluorescence (data not shown); however, using an anti-mCherry antibody, we were able to detect mCherry-positive cells in all tissues. Surprisingly, the number of mCherry-positive cells was low, with no detectable mCherry protein in the majority of cells. We then performed quantitative digital PCR (dPCR) using genomic DNA, with amplicons to measure both mCherry and the control RPP30 gene (**Fig. 3B**)³⁹. Because each diploid cell encodes two copies of RPP30, the ratio of mCherry (which should be a single copy/cell) to RPP30 can be used to calculate the number of cells encoding mCherry. These data demonstrate that in virtually all tissues, only 5-8% of cells encode the BETLE cassette, indicating that the animal is mosaic, consistent with the IHC findings. While the fraction of mCherry+ cells was surprisingly consistent across tissues, both bulk cells and sorted subsets, we identified enrichment of mCherry+ cells in liver non-parenchymal cells (NPCs), with ~20% of these cells encoding mCherry (**Fig. 3B**, left). Liver non-parenchymal cells are distinct from hepatocytes (parenchymal cells), and contain a mixture of liver sinusoidal endothelial cells, hepatic stellate cells, and multiple types of immune cells (e.g., Kupffer cells and lymphocytes)⁴⁰. Because we did not detect enrichment of mCherry in any sorted subsets from peripheral blood, this suggests non-immune NPCs are the source of this enrichment.

Increase in mCherry RNA expression after in vitro culture:

In addition to mosaicism in primary cells, we observed that the mCherry RNA level, which is under the control of the CAG promoter and expected to be high, was low. To better understand this discrepancy, we isolated primary fibroblasts from skin punch biopsies and hepatocytes from a liver biopsy and placed them in cell culture. After a matter of days, we were able to detect mCherry using fluorescent microscopy (**Fig. 4A and Fig. S1**). To independently verify this observation, we performed dPCR using cDNA from primary cultured and

non-cultured hepatocytes. The expression of mCherry was calculated as a ratio relative to RNA expression levels of the control RPP30 gene. These data revealed a 12–14-fold increase in mCherry expression in primary cultured cells relative to non-cultured cells (**Fig. 4B**).

Epigenetic silencing of mCherry expression in vivo, and epigenetic remodeling after in vitro culture:

Based on these data, which demonstrated that mCherry expression was minimal in primary cells, but restored after a brief period of cell culture, we hypothesized that epigenetic modifications account for the differential regulation of mCherry. To test this, we performed Assay for Transposase-Accessible Chromatin using sequencing (ATAC-seq) to measure the impact of cell culture on primary fibroblasts, contrasting early culture (P0) against cells passaged four additional times (P4). These data identified stark differences in the chromatin of BETLE after extended cell culture. In P0 cells, the BETLE insert is in a relatively inaccessible state, consistent with the limited mRNA detected in these cells (**Fig. 5A-B**). In contrast ATAC-seq revealed a much more open chromatin state across BETLE in P4 cells, which could explain the significant increase in mRNA expression and ability to detect mCherry in these cells. This provides a potential mechanism for our observations and underscores the importance of considering epigenetic regulation in the design of exogenous DNA constructs.

DISCUSSION

Genetically edited animal models are essential experimental platforms to understand the fundamental biological mechanisms and etiology of human disease. While gene editing of rodent and other small animal models has been used for decades, not all human biological processes are accurately modeled in more evolutionarily distant organisms. Gene editing of non-human primates, such as RMs, would enable a new generation of precise disease models to advance our understanding of disease and aid the development of novel therapies. In addition to this potential, human gene therapies will provide relief for previously incurable genetic conditions^{41,42}. These therapies will require robust animal models to ensure accurate delivery and editing.

While germline gene editing of RMs was first demonstrated in 2001, it remains extremely expensive and inefficient to generate genetically altered RMs, and relatively few have been generated in the subsequent decades. One of the major barriers to RM gene editing is the reduced oocyte production of RMs relative to rodents. It is therefore essential to maximize editing efficiency. Here we report the generation of a healthy transgenic RM encoding the Bivalent Enhanced Traffic Light Editing (BETLE) reporter, a previously characterized system that provides fluorescent readouts for on- and off-target gene editing³¹. The cassette was delivered by microinjection of plasmid DNA and piggyBac transposase mRNA, which resulted in random integration of the cassette. We performed genetic screening of embryos prior to implantation, selecting an embryo with a single copy of BETLE, integrated outside known genes, resulting in the birth of a healthy RM. The data and methods reported here, including pitfalls, represent key information to the developing field of RM gene editing.

While BETLE was encoded by cells of each germ layer, molecular and histologic analyses revealed mosaicism, with only 5-8% of cells encoding BETLE. Interestingly, the fraction of BETLE encoding cells was extremely consistent across diverse tissues, suggesting the integration event occurred very early in development. While the animal has not yet reached sexual maturity, these data strongly suggest sperm will also be mosaic. This raises the possibility of performing *in vitro* fertilization, screening the resulting embryos, and selectively transferring BETLE-encoding embryos to generate non-mosaic progeny.

In addition to mosaicism, the expression of mCherry mRNA and protein, which is expected to be constitutively expressed by BETLE, was lower than expected *in vivo*. Expression was recovered by culturing primary cells, and we further demonstrate that chromatin structure changes after culture, increasing accessibility of the BETLE promoter. This negative result nonetheless provides important information for the design of future transgenes. First, it may be useful to include chromatin insulators flanking an exogenous transgene⁴³. Second, these data emphasize the importance of the site of integration. We selected the randomly integrating piggyBac system for these experiments because it provides higher efficiency gene delivery than available site-directed methods, an essential feature when the number of oocytes is limited. If site-directed approaches could achieve transgene delivery with sufficient efficiency, these could offer major advantages for the creation of transgenic RMs.

While this RM is not suitable as an in vivo reporter of gene editing, the process of generating this RM and thorough genetic characterization provide important information for the nascent field of RM gene editing that will enhance gene delivery and transgene design.

Acknowledgements

This work was supported by the National Institutes of Health Somatic Cell Genome Editing U24OD026631 (to J.D.H.), R21OD037648 (to B.N.B. and B.J.B.), and the Office of the Director, National Institutes of Health P51OD011092 to the Oregon National Primate Research Center. This project uses resources supported by R24OD021324. The research reported in this publication used computational infrastructure supported by the Office of Research Infrastructure Programs, Office of the Director, of the National Institutes of Health under Award Number S10OD034224. It would not be possible without the Oregon National Primate Research Center Division of Comparative Medicine, the Endocrinology Services Core, and the Assisted Reproductive Core. The content is solely the responsibility of the authors and does not necessarily represent the official views of the National Institutes of Health.

Author Contributions

BNB, BJB, CBH, and JDH conceptualized the experiments and acquired funding. JR, KR, HN, JT, BH, SB, LNR, SY, BD, SMP, CBH, and BJB conducted experiments. JMW designed the BETLE construct used for microinjection and subcloned into the piggyBac vector. JR and BNB drafted the manuscript, and all authors contributed to editing.

Conflict of Interest

The authors declare they have no conflicts of interest.

METHODS

Animals: Rhesus macaques were socially housed at the Oregon National Primate Research Center (ONPRC) in animal biosafety level 2 rooms with autonomously controlled temperature, humidity, and lighting. Rhesus macaques were fed commercially prepared primate chow twice daily and received daily fresh fruit or vegetables. Fresh, potable water was provided via automatic water systems. Animal care and all experimental protocols and procedures were approved by the ONPRC Institutional Animal Care and Use Committee (IACUC), in accordance with relevant guidelines and regulations. The Laboratory Animal Care and Use Program at the ONPRC is fully accredited by the Association for Assessment and Accreditation of Laboratory Animal Care International. The ONPRC has a Category I approved assurance (no. A3304-01) for the care and use of animals on file with the National Institutes of Health Office for Protection from Research Risks. ONPRC adheres to national guidelines established in the Animal Welfare Act (7 U.S. Code, sections 2131–2159) and the *Guide for the Care and Use of Laboratory Animals, Eighth Edition* as mandated by the U.S. Public Health Service Policy.

Oocyte collection and in vitro fertilization (IVF): Oocyte collection and in vitro fertilization were performed as previously described³⁵. The ONPRC Assisted Reproductive Technologies (ART) Core provided gametes and performed *in vitro* fertilization (IVF) according to published protocols. Sexually mature rhesus monkeys with normal ovarian cyclicity were treated with a standard 10-day controlled ovarian stimulation cycle regimen as previously described to produce multiple pre-ovulatory follicles containing mature ova⁴⁴. Prior to ovulatory events, ultrasound-guided percutaneous follicle aspiration was performed, and recovered oocytes were isolated into warmed TALP-HEPES containing 0.3% bovine serum albumin with 5 IU/mL of heparin. Cumulus-enclosed metaphase II (MII) ova were washed into pre-equilibrated 100 μ L drops of BO-IVF (IVF Bioscience; Falmouth, Cornwall, UK) under oil with 5 ova/drop and incubated for approximately 4 hours at 37°C in humidified 5% CO₂ in air until insemination. Rhesus macaque semen was collected from a male on the same day as oocyte collection, and the sperm were washed in warmed TALP-HEPES to a final concentration of 20 million sperm/mL⁴⁵. A standard in vitro fertilization protocol was followed with sperm activated by 1 mM caffeine + 1 mM dibutyryl cAMP for 15 minutes before adding 10 μ l to each culture drop containing ova^{44,45}.

Injection of plasmid and PiggyBac mRNA into rhesus macaque zygotes: Microinjection was performed as previously described³⁵. Approximately 14 hours post-insemination, presumptive zygotes were washed to remove sperm attached to the zona pellucida and transferred into a warmed TALP-HEPES drop covered with oil. Injection material containing 30 or 100 ng/ μ L of piggyBac-compatible transgene plasmid, along with 30 ng/ μ L of piggyBac mRNA (Hera biolabs), was backloaded into a glass-pulled micro injection pipette. Zygotes were stabilized by gentle suction onto a glass holding pipette (Cooper Surgical), and material was injected under continuous positive flow into the cytoplasm of zygotes, using a Narishige micromanipulator (Narishige International, Amityville, NY). Injected embryos were then transferred into embryo culture media (BO-IVC, IVF Bioscience), covered with oil, and cultured in a 6%, 5%, 89% mixture of CO₂, O₂, and N₂ at 37°C in humidified air, respectively. The full sequence of the plasmid used for microinjection was submitted to Genbank under accession PX781468.

Trophectoderm (TE) cell biopsy from PiggyBac-injected blastocysts: Once embryos developed into expanded blastocysts, between days 7-9 post-insemination, a TE biopsy was performed as previously described^{35,46}. Briefly, individual blastocysts were placed in a 20 μ L drop of warmed TALP-HEPES under oil and stabilized with a holding pipette. An objective-mounted laser (ZYRCOS, Hamilton Thorne, Inc., Beverly, MA) was used to create a rent in the zona pellucida, creating an opening large enough to pass the glass biopsy pipette (Cooper Surgical) to aspirate TE cells following laser dissection of 10-15 cells. Biopsied TE cells were transferred into a PCR tube to conduct WGA and to identify the integration of the plasmid. Embryos are subjectively assessed before and during biopsy and graded as poor, medium, and good quality. Embryos are re-assessed after thawing, primarily based on re-expansion of the blastocoel. The biopsied blastocyst was then vitrified in a 0.25 cc straw (IMV Technologies, Maple Grove, MN) using the DMSO Blastocyst Vitrification Kit (LifeGlobal Group; Guildord, CT) according to the manufacturer's guidelines. Embryos that arrested during mitosis and failed to develop to the blastocyst stage underwent complete zona pellucida removal by brief exposure to acidic Tyrode's solution (prepared in-house according to⁴⁴) and were stored for subsequent analysis of transgene integration into the genome.

Embryo transplantation and pregnancy: The surrogate dam underwent laparotomy for embryo transplant into the oviduct, and pregnancy was confirmed via ultrasound 28 days post-transplant. Ultrasound was performed during the early second trimester (63 days post-transplant), indicating normal fetal growth assessed via biparietal diameter measurements⁴⁷. The surrogate dam was noted to have slow amniotic fluid leakage 138 days post-transplant. Fetal ultrasound was performed at 139 days post-transplant and revealed a healthy fetus with normal heart rate (170/min) and growth, but in breech position. Betamethasone was administered to the dam in the event of early delivery (0.25mg/kg IM on d138 and d139) along with prophylactic antibiotics to decrease the risk of ascending uterine infection to the fetus (azithromycin 40mg/kg/d x1d followed by 20mg/kg/d PO until delivery). Amoxicillin (8mg/kg PO BID) was also administered based on human obstetric guidelines but discontinued after 24 hrs due to the development of diarrhea in the dam⁴⁸. Enclosure side fetal ultrasound checks were performed every 1-2 days until delivery. The fetal heart rate remained normal, and the fetus was noted in vertex position for vaginal delivery by day 140. The fetus was delivered vaginally 147 days post embryo transplant without complications.

Enhanced Specificity Tagmentation-Assisted PCR (esTag-PCR): The esTag-PCR protocol was identical to the previously published protocol³⁵. For experiments with rhesus macaque embryos, TE biopsies were performed (described above), followed by WGA using REPLIg (Qiagen #150345), according to the manufacturer's instructions. The WGA product was purified using Ampure XP beads (Beckman Coulter) at a bead to sample ratio of 0.9. For experiments involving macaque tissues, genomic DNA was extracted using the Qiagen AllPrep DNA/RNA kit, according to the manufacturer's protocol. For esTag-PCR, the initial tagmentation step was performed with 100ng of gDNA or purified WGA product in a tagmentation reaction that included: 25 μ L TD buffer, 2.5 μ L Illumina TDE1 enzyme, 100 ng DNA, and H₂O to a final volume of 50 μ L. After preheating the thermocycler to 58° C, the reaction mixture was incubated for 5 min at 58° C, followed by a 10° C hold. The fragmented DNA was purified using Ampure XP beads with a 0.8 bead to sample ratio and eluted into 30 μ L H₂O. Following tagmentation, the first-round PCR was then performed using: 25 μ L KAPA HiFi HotStart ReadyMix (Kapa Biosystems KK2602), 1.25 μ L of each primer at 10 μ M (see Supplemental Table I of the original publication³⁵), and 21.25 μ L tagmentation product. The following PCR conditions were used: 95° C for 3 min, followed by 30 cycles of: 98° C for 30s, 63° C for 30s, and 72° C for 1 min, followed by 72° C for 10 min

and a 4° C hold. A secondary nested PCR was then performed using: 12.5 µL KAPA HiFi HotStart ReadyMix, 1.25 µL of index primer at 10µM, 0.75 µL of each transgene-specific primer at 10µM, 2 µL of the first-round PCR, and 7.5 µL H₂O. PCR conditions for the nested PCR were: 98° C for 45s, followed by 10 cycles of: 98° C for 20s, 54° C for 30s, and 72° C for 20s, ending with 72° C for 1 min and a 4° C hold. The second PCR adds a unique index to each sample. The PCR reaction was cleaned using Ampure XP beads at a 0.8 bead-to-sample ratio. Purified samples were quantified using a Qubit Fluorometer (Invitrogen). The resulting libraries were sequenced using Illumina chemistry. Integration site mapping was performed using the IntegrationSiteMapper tool available through the DISCVR-seq package^{35,49}.

PacBio Sequencing and Variant Calling: High molecular weight (HMW) genomic DNA was extracted from blood or tissue samples using the Gentra Puregene kit (Qiagen), with slight modifications to avoid shearing through sample pipetting or exposure to elevated temperatures. Extracted genomic DNA samples were sent to the University of Oregon Genomics & Cell Characterization Core Facility, which performed standard quality control procedures to verify samples met with DNA length requirements prior to library preparation. Libraries were sequenced on a PacBio Sequel II system, using one SMRT cell 8M per library. Samples were sequenced using CCS chemistry. Raw data have been deposited into the NIH SRA Database, under accession # SRR31943588. The resulting sequence data were aligned to the MMuL_10 reference genome (GCA_003339765.3) augmented with a contig for the BETLE cassette (GenBank Accession: OK480061), using pbmm2 (version 1.17.0). CCS data were aligned with the option `--preset=CCS`. To call variants with pbsv, the command 'pbsv discover' was run per sample with default parameters, followed by 'pbsv call' with the argument `--ccs` supplied. Short variants were called from the PacBio data using DeepVariant⁵⁰.

PCR amplification and short-read sequence validation of the BETLE insert: The chromosomal region of the BETLE cassette insertion site identified by esTag-PCR (chromosome 5, position 47,727,101) was amplified as three amplicons, in part to overcome the high GC content of the CAG promoter region. All PCR reactions were performed in a 25 µL volume using KAPA HiFi HotStart ReadyMix (Roche) with DMSO supplementation at a final concentration of 5%, and primers at a final concentration of 0.3 µM. The 5' portion of BETLE and the CAG

promoter region were amplified using nested-PCR. The first PCR for both targets was performed using primers 5'-TCAGTAGATAATTATGACGGCAATAATCCAC and 5'-GGTGCCGTAGTGCAGGATCAC, with 12.5 ng of gDNA as a template. The PCR conditions were as follows: initial denaturation at 95 °C for 5 min, followed by 35 cycles of 98 °C for 20 sec, 60°C for 15 sec, and 72°C for 4 min with a final extension at 72°C for 2 min. One nested PCR reaction was performed using 1 µL of the first PCR products as a template, with the same conditions except for an annealing temperature of 65°C instead of 60°C, with primers: 5'-CGTTTCTGCCTTCCAGGCCAC and 5'-CATGCTCTATATATTACCATAAACATTCGTTAC. A second nested PCR reaction was performed to ensure complete coverage of the CAG promoter region, using 1 µL of the first PCR products as a template, with the same conditions except for an annealing temperature of 65°C instead of 60°C, and extension time of 2 minutes, using primers: 5'-CATGCTCTATATATTACCATAAACATTCGTTAC and 5'-GGTACCGTCGACTGCAGAAT. The 3' portion of the BETLE cassette was amplified by a single-step PCR using primers: 5'-CGTGAACCTCACCTCCAACGG and 5'-CTATGAATAGTATAGAACCCTACAAATACATAC. The PCR conditions were initial denaturation at 98°C for 30 sec, followed by 35 cycles of 98 °C for 10 sec, 60 °C for 30 sec, and 72 °C for 1.5 min, with a final extension at 72 °C for 5 min. The PCR fragments were gel-extracted by QIAquick Gel Extraction Kit (Qiagen), and Illumina libraries were constructed using the Nextera XT DNA Library Preparation Kit (Illumina) following the manufacturer's instructions. Library quality, quantity and fragment sizes were assessed using an Agilent Bioanalyzer 2100 high-sensitivity DNA chip. Sequencing was performed using an Illumina MiSeq, v2 kit (300-cycles), operated by the ONPRC Primate Genetics Core. Raw data have been deposited into the NIH SRA Database, under BioProject PRJNA1359011. The accession numbers of each dataset are listed in Table S2.

Skin biopsy and fibroblast cell isolation: Under sedation, skin biopsies were collected from the transgenic RM and a control wild-type RM. The skin biopsy samples were washed twice with ice-cold phosphate-buffered saline (PBS) supplemented with 2x antibiotics. The washed skin tissue was then minced into small pieces and incubated at 37°C with Liberase TM (Roche, 5401119001) for 30 minutes in a humidified incubator with 5% CO₂. After digestion, the samples were washed twice with Dulbecco's Modified Eagle Medium containing 15% fetal bovine serum and GlutaMAX supplement. The tissue was then transferred to a 6-well tissue culture plate and cultured at 37°C until cells reached approximately 80% confluency.

Laparoscopic liver partial lobectomy: An approximately 2/3 partial lobectomy of the left lateral lobe of the liver was performed as described previously^{29,51,52} with the following changes to permit the larger sample collection through three 5 mm ports. The rhesus macaque was in dorsal recumbency, the camera port was placed caudal to the umbilicus, and the two midabdominal instrument ports were placed approximately 2-3 cm off midline on each side. A Caiman 5 Vessel Sealer was used to perform the partial lobectomy, followed by the removal of the liver tissue from the abdomen in a tissue bag to avoid damaging the sample.

Isolation of rhesus macaque primary hepatocytes: The biopsied left lateral liver lobe was placed in a petri dish, and a catheter (Introcan Safety 20G IV Catheter, Cat# 4251644) was inserted into the exposed vein and adhered using surgical glue. Tubing that had been flushed with Pre-Perfusion Media consisting of HBSS -/- (Fisher Scientific, Cat# MT21021CV), 0.1% 0.5M EGTA (Bioworld, Cat# 40520008), 0.5% 10 IU/mL Heparin (NDC# 63323-540-33) was attached to the catheter and fed through a Masterflex L/S Easy-Load peristaltic pump (ColePalmer, Cat# 77200-50). The other end of the tubing was placed in a beaker containing Pre-Perfusion Media, and the pump was turned on at a rate of 40 mL/min, with the media perfused through the lobe into the petri dish being aspirated during the process. Once 250 mL of Pre-Perfusion Media had been pumped through the lobe, the tubing was moved to a new beaker containing 250 mL HBSS +/- (ThermoFisher, Cat# 24020117). The pump was set to a flow rate of 40 mL/min, and once all 250 mL of HBSS +/- was pumped through the lobe, the pump was turned off. 150 mL Collagenase Base Buffer (HBSS +/-, 0.5 mM EGTA, 25 IU Heparin) was added to the beaker and placed in a 37°C water bath. The pump was turned on at a rate of 40 mL/min and once 50 mL of Collagenase Base Buffer was pumped through the lobe, the pump was stopped, and 25 mg NB4 Collagenase (Crescent Chemical, Cat# 17465) was added to the beaker. The liver lobe was removed from the petri dish and placed in the beaker containing the Collagenase Buffer Solution, creating a closed-loop system. The pump was turned on at a rate of 40 mL/min for 40 minutes. After incubation, the liver was removed from the water bath, gently probed with forceps, and dissected with scalpels. The liver solution was filtered through a 100 µm filter and the filtrate was centrifuged at 50 × g for 3 minutes. The pellet was washed twice in Cell Culture Media consisting of DMEM-F12 (Fisher Scientific, Cat# 11-320-082), 10% heat-inactivated fetal bovine serum (Neuromics, Cat# FBS002), 1% antibiotic/antimycotic solution (Fisher Scientific, Cat# SV30079.01), 1% L-

Glutamine (ThermoFisher, Cat# 25030081), and 1% sodium pyruvate (Fisher Scientific, Cat# SH3023901), and then centrifuged at 50 × g for 3 minutes. The pellet was resuspended in Cell Culture Media and filtered through a 70 µm filter, then centrifuged at 50 × g for 3 minutes. The pellet was resuspended in ACK Lysis Buffer and incubated at room temperature for 5 minutes. The sample solution was washed twice with 10 mL of Cell Culture Media and centrifuged at 350 × g for 5 minutes. The hepatocytes were resuspended in Cell Culture Media, quantified and used for further experiments.

Digital PCR (dPCR) for detection of mCherry DNA and RNA: Genomic DNA and RNA were extracted from cells using the Qiagen AllPrep DNA/RNA kit following the manufacturer's protocol. From the RNA, first-strand cDNA was generated using SuperScript IV Vilo Master Mix with ezDNase following the manufacturer's protocol. Copy numbers of the mCherry and RPP30 (internal control) genes/cDNAs were determined by duplex digital PCR using the QuantStudio Absolute Q Digital PCR System (Applied Biosystems, Thermo Fisher Scientific, Cat. A52864). The following primers and probes (synthesized by IDT) were used to amplify regions of the mCherry and RPP30 sequences: for mCherry, forward primer 5'-GAGGCTCAAGCTCAAGGAC-3', reverse primer 5'-GATGGTGTAGTCCTCGTTGTG-3', and probe 5'-CCAAGTGGATGTTGACGTTGTAGGCG-3'; for RPP30, forward primer 5'-AGGATGCTCCGGGAGTATGTA-3', reverse primer 5'-CCTGCTTGTCACCTATATAACAT-3', and probe 5'-/5SUN/TCAAGCTGG/ZEN/GAGACGGAAGAGTCAGT/3IABkFQ/-. PCR reaction mixtures were prepared using the QuantStudio Absolute Q Universal DNA Master Mix (Applied Biosystems, Thermo Fisher Scientific, Cat. A72710) and loaded onto MAP16 Digital PCR Plates (Applied Biosystems, Thermo Fisher Scientific, Cat. A52865) according to the manufacturer's instructions. Thermal cycling was performed using the TaqMan Copy Number Assay conditions: 96 °C for 10 min, followed by 40 cycles of 98 °C for 15 s and 60 °C for 30 s.

Flow cytometry (FACS) analysis: For FACS analysis, 1 × 10⁶ cells (0.5 × 10⁶ cells for hepatocytes) were added to flow tubes and washed once with 1 × PBS, then spun at 350 × g for 5 minutes. Supernatants were aspirated and tubes were vortexed. A surface stain antibody cocktail was added to each tube at 50 µL each (CD45 PE-Cy7 BD Biosciences Cat# 561294, and Fixable Viability Stain 575V BD Biosciences Cat#565694). Tubes were

incubated for 20 minutes at room temperature in the dark. After the incubation, tubes were washed once with 1 × PBS, then spun at 350 × g for 5 minutes. Supernatants were aspirated, and tubes were vortexed. Cells were then fixed with eBioscience™ Foxp3 / Transcription Factor Fixation Buffer diluted 1:4 with kit-provided dilution buffer. Tubes were incubated for 20 minutes at room temperature in the dark. After the incubation, tubes were washed once with kit-provided permeabilization buffer, then spun at 830 × g for 4 minutes. Supernatants were aspirated and tubes were vortexed, then rabbit α-mCherry primary antibody (Abcam Cat# ab167453) diluted 1:500 in eBioscience™ permeabilization buffer was added to each tube. Tubes were incubated for 40 minutes at room temperature in the dark. After the incubation, tubes were washed once with kit-provided permeabilization buffer, then spun at 830 × g for 4 minutes. Supernatants were aspirated and tubes were vortexed, then α-rabbit IgG AF647 secondary antibody (Invitrogen Cat# A32795) diluted 1:200 in eBioscience™ permeabilization buffer was added to each tube. Tubes were incubated for 40 minutes at room temperature in the dark. After the incubation, tubes were washed once with kit-provided permeabilization buffer, then spun at 830 × g for 4 minutes. Tubes were then washed with FACS buffer (1 × PBS supplemented with 2% FBS), then spun at 830 × g for 4 minutes. Supernatants were aspirated and tubes were vortexed, then flow cytometric analysis was performed on an A5 instrument running FACSDiva software v8.0 (BD Biosciences). Analysis was performed using FlowJo software v10.8.1 (Tree Star).

Microscopy of Primary Hepatocytes: Primary hepatocytes (PH) were plated at a density of 1×10^6 cells/well on cell culture–treated flat-bottom microplates (Fisher Scientific, Cat# 08-772-3) coated with rat-tail collagen at 300 µg/mL (Fisher Scientific, Cat# A1048301). On days 1, 4, 7, and 11 post-plating, wells were washed once with 1 × PBS and then visualized on a BZ-X810 Series Keyence Fluorescence Microscope under brightfield (1/2800 second exposure time) and BZ-X Filter TexasRed filter cube (¼ second exposure time).

mCherry detection in tissues using immunohistochemistry (IHC): For immunohistochemistry studies, tissue sections were fixed in 4% paraformaldehyde, processed for paraffin embedding, and cut at 7 µm thickness. The slides were de-waxed in xylene, rehydrated in graded ethanol, and then subjected to antigen retrieval in citraconic anhydride (CA) solution (Sigma) 0.1M, pH 6.0 for 15 min at 110 °C and 5 psi. Slides were cooled,

washed with water, and then incubated with an anti-mCherry rabbit polyclonal antibody (Abcam, Cat# ab167453) diluted to 1:200 in Tris-buffered saline (TBS; containing 0.05% Tween-20, 0.01 M, PH 7.4) for 1 h at room temperature. Slides were washed with TBS-T for 5 min and then incubated with 1.5% hydrogen peroxide solution (Fisher, Cat# H325-500) diluted in TBS-T for 5 min to dissolve all endogenous peroxide and then incubated with two drops of HRP-conjugated anti-rabbit secondary antibody (Origene, Cat# D13-110) for 20 min at room temperature. Slides were washed in TBS-T for 5 min and developed with 3,3'-diaminobenzidine (Vector Laboratories, Cat# SK-4105) and counterstained with Hematoxylin (Vector Laboratories Cat# H-3404-100). Slides were dehydrated in graded ethanol and xylene, mounted in Permount (Fisher Scientific, Cat# SP15-100), and cover-slipped. Images were acquired by scanning the entire tissue at $\times 40$ magnification using an Olympus VS120 Slide Scanner and analyzed using the CellSens™ Dimension Desktop v1.18 software (Olympus).

Assay for Transposase-Accessible Chromatin using sequencing (ATAC-seq): To assess chromatin

accessibility, ATAC-seq was performed. The following reagents were prepared the day of the experiment: resuspension buffer (RSB) consisting of 10mM Tris-HCL (pH 7.4), 10mM NaCl and 3mM MgCl₂, in nuclease-free water; wash buffer consisting of RSB and 0.1% Tween-20; lysis buffer consisting of RSB 0.1% Tween-20, 0.1% IGEPAL-CA-630, and 0.001% Digitonin; and transposition mix consisting of 25 μ L 2x TD buffer, 2.5 μ L TDE1, and 22.5 μ L lysis buffer. 2x TD buffer and TDE enzyme were obtained from the Tagment DNA Enzyme and Buffer Kit (Illumina). A total of 1.5×10^5 cells were collected, washed with 1X PBS, and centrifuged at 500 x g for 5 min at 4°C. To begin nuclei preparation, the supernatant was discarded and 5.0×10^4 cells were resuspended in each of three aliquots of 1 mL ice-cold PBS and centrifuged at 500 x g for 5 min at 4°C. The supernatant was discarded, and the cell pellet was resuspended in 50 μ L of Lysis Buffer and incubated on ice for 3 minutes. During this step, efficient cell membrane disruption and preservation of nuclear integrity were confirmed by Trypan Blue staining and light microscopy. Next, 1 mL of ice-cold wash buffer was added, the samples inverted to mix, then centrifuged at 500 x g for 10 min at 4°C. The supernatant was again discarded, the cell pellet placed on ice, resuspended in 50 μ L transposition mix, gently mixed by pipetting, then incubated at 37°C for 30 min mixing at 1000 rpm with the Eppendorf ThermoMixer F1.5. After the 30-minute mix, the transposition reaction was purified using the Qiagen MinElute Reaction Cleanup kit following the manufacturer's protocol. To amplify transposed DNA fragments the following were combined in a 0.2 mL PCR

tube: 10 μ L transposed DNA, 10 μ L nuclease-free water, 2.5 μ L 25uM Nextera PCR primer 1, 2.5 μ L 25uM Nextera PCR primer 2, and 25 μ L NEBNext High-Fidelity 2x PCR Master Mix. Samples were then partially amplified using the following program on the Applied Biosystems VeritiPro 96-well Thermal Cycler: 72°C for 5 minutes, 98°C for 30 seconds, followed by 5 cycles of 98°C for 10 seconds, 63°C for 30 seconds, and 72°C for 1 minute. Reaction tubes were placed on ice, and 5 μ L of each partially amplified library along with nuclease-free water, Nextera PCR primers 1 & 2, SYBR Green I, and NEBNext High-Fidelity 2x Master Mix, were used to perform qPCR on the Applied Biosystems QuantStudio 3 to determine how many additional PCR cycles were needed to stop amplification prior to saturation. The following program was run on the QuantStudio 3: 98°C for 30 seconds, followed by 20 cycles of 98°C for 10 seconds, 63°C for 30 seconds, and 72°C for 1 minute. After 20 cycles, the additional number of cycles was determined by plotting linear Rn versus cycle and determining the cycle number corresponding to one quarter of maximum fluorescent intensity. The remaining 45 μ L of partially amplified library was then run for N cycles, N being the cycle number determined by qPCR, on the VeritiPro 96-well Thermal Cycler using a program similar to the initial PCR, excluding the 5 minutes at 72°C. Library purification was performed using AMPure XP beads and a double-sided purification protocol, and sample quality was assessed using the Agilent 2100 Bioanalyzer System. Samples were then aliquoted and sequenced using Illumina chemistry. Raw sequence data from ATAC-seq libraries were aligned to the MMul_10 reference genome (GCA_0033339765.3), augmented with a contig for the BETLE cassette (GenBank Accession: OK480061), using bwa mem⁵³. Per sample, peaks were called using Genrich⁵⁴, run using default parameters. Identical ATAC-seq samples from a control wild-type macaque were generated, and these triplicate libraries were used as the control sample when running Genrich. Raw data have been deposited into the NIH SRA Database, under BioProject PRJNA1359011. The accession numbers of each dataset are listed in Table S2.

LITERATURE CITED

1. Phillips, K.A., Bales, K.L., Capitanio, J.P., Conley, A., Czoty, P.W., Hart, B.A., Hopkins, W.D., Hu, S.L., Miller, L.A., Nader, M.A., et al. (2014). Why primate models matter. *Am J Primatol* 76, 801-827. 10.1002/ajp.22281.
2. Vallender, E.J., Hotchkiss, C.E., Lewis, A.D., Rogers, J., Stern, J.A., Peterson, S.M., Ferguson, B., and Sayers, K. (2023). Nonhuman primate genetic models for the study of rare diseases. *Orphanet J Rare Dis* 18, 20. 10.1186/s13023-023-02619-3.

3. Cornish, A.S., Gibbs, R.M., and Norgren, R.B., Jr. (2016). Exome screening to identify loss-of-function mutations in the rhesus macaque for development of preclinical models of human disease. *BMC genomics* *17*, 170. 10.1186/s12864-016-2509-5.
4. Isakova, I.A., Baker, K.C., Dufour, J., and Phinney, D.G. (2017). Mesenchymal Stem Cells Yield Transient Improvements in Motor Function in an Infant Rhesus Macaque with Severe Early-Onset Krabbe Disease. *Stem Cells Transl Med* *6*, 99-109. 10.5966/sctm.2015-0317.
5. Ishiwata, A., Mimuro, J., Mizukami, H., Kashiwakura, Y., Yasumoto, A., Sakata, A., Ohmori, T., Madoiwa, S., Ono, F., Shima, M., et al. (2010). Mutant macaque factor IX T262A: a tool for hemophilia B gene therapy studies in macaques. *Thromb Res* *125*, 533-537. 10.1016/j.thromres.2010.01.049.
6. Guggino, W.B., Benson, J., Seagrave, J., Yan, Z., Engelhardt, J., Gao, G., Conlon, T.J., and Cebotaru, L. (2017). A Preclinical Study in Rhesus Macaques for Cystic Fibrosis to Assess Gene Transfer and Transduction by AAV1 and AAV5 with a Dual-Luciferase Reporter System. *Hum Gene Ther Clin Dev* *28*, 145-156. 10.1089/humc.2017.067.
7. Gyorgy, B., Meijer, E.J., Ivanchenko, M.V., Tenneson, K., Emond, F., Hanlon, K.S., Indzhukulian, A.A., Volak, A., Karavitaki, K.D., Tamvakologos, P.I., et al. (2019). Gene Transfer with AAV9-PHP.B Rescues Hearing in a Mouse Model of Usher Syndrome 3A and Transduces Hair Cells in a Non-human Primate. *Mol Ther Methods Clin Dev* *13*, 1-13. 10.1016/j.omtm.2018.11.003.
8. McBride, J.L., Neuringer, M., Ferguson, B., Kohama, S.G., Tagge, I.J., Zweig, R.C., Renner, L.M., McGill, T.J., Stoddard, J., Peterson, S., et al. (2018). Discovery of a CLN7 model of Batten disease in non-human primates. *Neurobiol Dis* *119*, 65-78. 10.1016/j.nbd.2018.07.013.
9. Francis, P.J., Appukuttan, B., Simmons, E., Landauer, N., Stoddard, J., Hamon, S., Ott, J., Ferguson, B., Klein, M., Stout, J.T., and Neuringer, M. (2008). Rhesus monkeys and humans share common susceptibility genes for age-related macular disease. *Hum Mol Genet* *17*, 2673-2680. 10.1093/hmg/ddn167.
10. Moshiri, A., Chen, R., Kim, S., Harris, R.A., Li, Y., Raveendran, M., Davis, S., Liang, Q., Pomerantz, O., Wang, J., et al. (2019). A nonhuman primate model of inherited retinal disease. *J Clin Invest* *129*, 863-874. 10.1172/JCI123980.
11. Bimber, B.N., Ramakrishnan, R., Cervera-Juanes, R., Madhira, R., Peterson, S.M., Norgren, R.B., Jr., and Ferguson, B. (2017). Whole genome sequencing predicts novel human disease models in rhesus macaques. *Genomics* *109*, 214-220. 10.1016/j.ygeno.2017.04.001.
12. Bimber, B.N., Yan, M.Y., Peterson, S.M., and Ferguson, B. (2019). mGAP: the macaque genotype and phenotype resource, a framework for accessing and interpreting macaque variant data, and identifying new models of human disease. *BMC Genomics* *20*, 176. 10.1186/s12864-019-5559-7.
13. Fawcett, G.L., Raveendran, M., Deiros, D.R., Chen, D., Yu, F., Harris, R.A., Ren, Y., Muzny, D.M., Reid, J.G., Wheeler, D.A., et al. (2011). Characterization of single-nucleotide variation in Indian-origin rhesus macaques (*Macaca mulatta*). *BMC Genomics* *12*, 311. 10.1186/1471-2164-12-311.
14. Massaro, G., Mattar, C.N.Z., Wong, A.M.S., Sirka, E., Buckley, S.M.K., Herbert, B.R., Karlsson, S., Perocheau, D.P., Burke, D., Heales, S., et al. (2018). Fetal gene therapy for neurodegenerative disease of infants. *Nat Med* *24*, 1317-1323. 10.1038/s41591-018-0106-7.
15. Liang, W., He, J., Mao, C., Yu, C., Meng, Q., Xue, J., Wu, X., Li, S., Wang, Y., and Yi, H. (2022). Gene editing monkeys: Retrospect and outlook. *Front Cell Dev Biol* *10*, 913996. 10.3389/fcell.2022.913996.
16. Yang, S.H., Cheng, P.H., Banta, H., Piotrowska-Nitsche, K., Yang, J.J., Cheng, E.C., Snyder, B., Larkin, K., Liu, J., Orkin, J., et al. (2008). Towards a transgenic model of Huntington's disease in a non-human primate. *Nature* *453*, 921-924. 10.1038/nature06975.
17. Park, J.E., and Silva, A.C. (2019). Generation of genetically engineered non-human primate models of brain function and neurological disorders. *Am J Primatol* *81*, e22931. 10.1002/ajp.22931.

18. Sato, K., and Sasaki, E. (2018). Genetic engineering in nonhuman primates for human disease modeling. *J Hum Genet* 63, 125-131. 10.1038/s10038-017-0351-5.
19. Chen, Y., Zheng, Y., Kang, Y., Yang, W., Niu, Y., Guo, X., Tu, Z., Si, C., Wang, H., Xing, R., et al. (2015). Functional disruption of the dystrophin gene in rhesus monkey using CRISPR/Cas9. *Hum Mol Genet* 24, 3764-3774. 10.1093/hmg/ddv120.
20. Seita, Y., Tsukiyama, T., Azami, T., Kobayashi, K., Iwatani, C., Tsuchiya, H., Nakaya, M., Tanabe, H., Hitoshi, S., Miyoshi, H., et al. (2019). Comprehensive evaluation of ubiquitous promoters suitable for the generation of transgenic cynomolgus monkeys. *Biol Reprod* 100, 1440-1452. 10.1093/biolre/iox040.
21. Seita, Y., Morimura, T., Watanabe, N., Iwatani, C., Tsuchiya, H., Nakamura, S., Suzuki, T., Yanagisawa, D., Tsukiyama, T., Nakaya, M., et al. (2020). Generation of Transgenic Cynomolgus Monkeys Overexpressing the Gene for Amyloid-beta Precursor Protein. *J Alzheimers Dis* 75, 45-60. 10.3233/JAD-191081.
22. Shi, L., Luo, X., Jiang, J., Chen, Y., Liu, C., Hu, T., Li, M., Lin, Q., Li, Y., Huang, J., et al. (2019). Transgenic rhesus monkeys carrying the human MCPH1 gene copies show human-like neoteny of brain development. *Natl Sci Rev* 6, 480-493. 10.1093/nsr/nwz043.
23. Chan, A.W., Chong, K.Y., Martinovich, C., Simerly, C., and Schatten, G. (2001). Transgenic monkeys produced by retroviral gene transfer into mature oocytes. *Science* 291, 309-312. 10.1126/science.291.5502.309.
24. Yang, W., Liu, Y., Tu, Z., Xiao, C., Yan, S., Ma, X., Guo, X., Chen, X., Yin, P., Yang, Z., et al. (2019). CRISPR/Cas9-mediated PINK1 deletion leads to neurodegeneration in rhesus monkeys. *Cell Res* 29, 334-336. 10.1038/s41422-019-0142-y.
25. Ryu, J., Statz, J.P., Chan, W., Oyama, K., Custer, M., Wienisch, M., Chen, R., Hanna, C.B., and Hennebold, J.D. (2024). Generation of Rhesus Macaque Embryos with Expanded CAG Trinucleotide Repeats in the Huntingtin Gene. *Cells* 13. 10.3390/cells13100829.
26. Yao, X., Liu, Z., Wang, X., Wang, Y., Nie, Y.H., Lai, L., Sun, R., Shi, L., Sun, Q., and Yang, H. (2018). Generation of knock-in cynomolgus monkey via CRISPR/Cas9 editing. *Cell Res* 28, 379-382. 10.1038/cr.2018.9.
27. Park, F. (2007). Lentiviral vectors: are they the future of animal transgenesis? *Physiol Genomics* 31, 159-173. 10.1152/physiolgenomics.00069.2007.
28. Picanco-Castro, V., de Sousa Russo-Carbolante, E.M., and Tadeu Covas, D. (2012). Advances in lentiviral vectors: a patent review. *Recent Pat DNA Gene Seq* 6, 82-90.
29. Rust, L.N., Wettengel, J.M., Biswas, S., Ryu, J., Piekarski, N., Yusova, S., Lutz, S.S., Naldiga, S., Hinrichs, B.J., Sullivan, M.N., et al. (2025). Liver-specific transgenic expression of human NTCP in rhesus macaques confers HBV susceptibility on primary hepatocytes. *Proc Natl Acad Sci U S A* 122, e2413771122. 10.1073/pnas.2413771122.
30. Nakaya, M., Iwatani, C., Tsukiyama-Fujii, S., Mieda, A., Tarumoto, S., Tsujimura, T., Yamamoto, T., Ichikawa, T., Nakamura, T., Terakado, I., et al. (2025). Non-viral generation of transgenic non-human primates via the piggyBac transposon system. *Nat Commun* 16, 2179. 10.1038/s41467-025-57365-w.
31. Wettengel, J.M., Hansen-Palmus, L., Yusova, S., Rust, L., Biswas, S., Carson, J., Ryu, J., Bimber, B.N., Hennebold, J.D., and Burwitz, B.J. (2023). A Multifunctional and Highly Adaptable Reporter System for CRISPR/Cas Editing. *Int J Mol Sci* 24. 10.3390/ijms24098271.
32. Cadinanos, J., and Bradley, A. (2007). Generation of an inducible and optimized piggyBac transposon system. *Nucleic Acids Res* 35, e87. 10.1093/nar/gkm446.
33. Kebriaei, P., Izsvak, Z., Narayanavari, S.A., Singh, H., and Ivics, Z. (2017). Gene Therapy with the Sleeping Beauty Transposon System. *Trends Genet* 33, 852-870. 10.1016/j.tig.2017.08.008.
34. Sandoval-Villegas, N., Nurieva, W., Amberger, M., and Ivics, Z. (2021). Contemporary Transposon Tools: A Review and Guide through Mechanisms and Applications of Sleeping Beauty, piggyBac and Tol2 for Genome Engineering. *Int J Mol Sci* 22. 10.3390/ijms22105084.

35. Ryu, J., Chan, W., Wettengel, J.M., Hanna, C.B., Burwitz, B.J., Hennebold, J.D., and Bimber, B.N. (2022). Rapid, accurate mapping of transgene integration in viable rhesus macaque embryos using enhanced-specificity tagmentation-assisted PCR. *Mol Ther Methods Clin Dev* 24, 241-254. 10.1016/j.omtm.2022.01.009.
36. Vilarino, M., Suchy, F.P., Rashid, S.T., Lindsay, H., Reyes, J., McNabb, B.R., van der Meulen, T., Huising, M.O., Nakauchi, H., and Ross, P.J. (2018). Mosaicism diminishes the value of pre-implantation embryo biopsies for detecting CRISPR/Cas9 induced mutations in sheep. *Transgenic Res* 27, 525-537. 10.1007/s11248-018-0094-x.
37. Ryu, J., Statz, J.P., Chan, W., Burch, F.C., Brigande, J.V., Kempton, B., Porsov, E.V., Renner, L., McGill, T., Burwitz, B.J., et al. (2022). CRISPR/Cas9 editing of the MYO7A gene in rhesus macaque embryos to generate a primate model of Usher syndrome type 1B. *Sci Rep* 12, 10036. 10.1038/s41598-022-13689-x.
38. Wilm, A., Aw, P.P., Bertrand, D., Yeo, G.H., Ong, S.H., Wong, C.H., Khor, C.C., Petric, R., Hibberd, M.L., and Nagarajan, N. (2012). LoFreq: a sequence-quality aware, ultra-sensitive variant caller for uncovering cell-population heterogeneity from high-throughput sequencing datasets. *Nucleic Acids Res* 40, 11189-11201. 10.1093/nar/gks918.
39. Wu, J., Yu, S., Wang, Y., Zhu, J., and Zhang, Z. (2022). New insights into the role of ribonuclease P protein subunit p30 from tumor to internal reference. *Front Oncol* 12, 1018279. 10.3389/fonc.2022.1018279.
40. Yang, T., Gu, Z., Feng, J., Shan, J., Qian, C., and Zhuang, N. (2025). Non-parenchymal cells: key targets for modulating chronic liver diseases. *Front Immunol* 16, 1576739. 10.3389/fimmu.2025.1576739.
41. Weuring, W., Geerligs, J., and Koeleman, B.P.C. (2021). Gene Therapies for Monogenic Autism Spectrum Disorders. *Genes (Basel)* 12. 10.3390/genes12111667.
42. Khanani, A.M., Thomas, M.J., Aziz, A.A., Weng, C.Y., Danzig, C.J., Yiu, G., Kiss, S., Waheed, N.K., and Kaiser, P.K. (2022). Review of gene therapies for age-related macular degeneration. *Eye (Lond)* 36, 303-311. 10.1038/s41433-021-01842-1.
43. Papayanni, P.G., Psatha, N., Christofi, P., Li, X.G., Melo, P., Volpin, M., Montini, E., Liu, M., Kaltsounis, G., Yiangou, M., et al. (2021). Investigating the Barrier Activity of Novel, Human Enhancer-Blocking Chromatin Insulators for Hematopoietic Stem Cell Gene Therapy. *Hum Gene Ther* 32, 1186-1199. 10.1089/hum.2021.142.
44. Ramsey, C., and Hanna, C. (2019). In Vitro Culture of Rhesus Macaque (*Macaca mulatta*) Embryos. *Methods Mol Biol* 2006, 341-353. 10.1007/978-1-4939-9566-0_23.
45. Houser, L.A., Ramsey, C., de Carvalho, F.M., Kolwitz, B., Naito, C., Coleman, K., and Hanna, C.B. (2021). Improved Training and Semen Collection Outcomes Using the Closed Box Chair for Macaques. *Animals (Basel)* 11. 10.3390/ani11082384.
46. McArthur, S.J., Leigh, D., Marshall, J.T., de Boer, K.A., and Jansen, R.P. (2005). Pregnancies and live births after trophoctoderm biopsy and preimplantation genetic testing of human blastocysts. *Fertil Steril* 84, 1628-1636. 10.1016/j.fertnstert.2005.05.063.
47. Tarantal, A.F., and Hendrickx, A.G. (1988). Prenatal growth in the cynomolgus and rhesus macaque (*Macaca fascicularis* and *Macaca mulatta*): A comparison by ultrasonography. *Am J Primatol* 15, 309-323. 10.1002/ajp.1350150405.
48. Prelabor Rupture of Membranes: ACOG Practice Bulletin, Number 217. (2020). *Obstet Gynecol* 135, e80-e97. 10.1097/AOG.0000000000003700.
49. DISCVR-Seq. DISCVR-Seq: A set of command line tools for working with sequence data. <https://bimberlab.github.io/DISCVRSeq/>.
50. Poplin, R., Chang, P.C., Alexander, D., Schwartz, S., Colthurst, T., Ku, A., Newburger, D., Dijamco, J., Nguyen, N., Afshar, P.T., et al. (2018). A universal SNP and small-indel variant caller using deep neural networks. *Nat Biotechnol* 36, 983-987. 10.1038/nbt.4235.
51. Moats, C., Cook, K., Armantrout, K., Crank, H., Uttke, S., Maher, K., Bochart, R.M., Lawrence, G., Axthelm, M.K., and Smedley, J.V. (2022). Antimicrobial prophylaxis does not improve post-surgical outcomes in SIV/SHIV-uninfected or SIV/SHIV-infected macaques (*Macaca mulatta*

- and *Macaca fascicularis*) based on a retrospective analysis. *PLoS One* 17, e0266616. 10.1371/journal.pone.0266616.
52. Zevin, A.S., Moats, C., May, D., Wangari, S., Miller, C., Ahrens, J., Iwayama, N., Brown, M., Bratt, D., Klatt, N.R., and Smedley, J. (2017). Laparoscopic Technique for Serial Collection of Liver and Mesenteric Lymph Nodes in Macaques. *J Vis Exp.* 10.3791/55617.
 53. Li, H., and Durbin, R. (2010). Fast and accurate long-read alignment with Burrows-Wheeler transform. *Bioinformatics* 26, 589-595. 10.1093/bioinformatics/btp698.
 54. Genrich: detecting sites of genomic enrichment. (2021). <https://github.com/jsh58/Genrich>.

FIGURE LEGENDS

Figure 1: BETLE construct and editing efficiency. **A)** Schematic of the BETLE expression construct, which was cloned into a plasmid vector flanked by piggyBac terminal repeat (TR) sequences. **B)** The graph summarizes the efficiency of oocyte isolation, fertilization, and genomic editing. **C)** The graph summarizes the number of BETLE integration events per embryo, which includes blastocysts and arrested embryos.

Figure 2: Genetic analysis of BETLE integration across tissues in a transgenic RM. **A)** Photo of transgenic RM at seven days of age. **B)** A schematic representing the genomic locations of BETLE integration events using material from either a trophectoderm biopsy from the embryo (top) or postnatal biopsies from the indicated tissues. **C)** A schematic of the BETLE construct, indicating the location of the PCR amplicons used for sequence validation.

Figure 3: mCherry protein expression and mosaicism in tissues. **A)** Immunohistochemistry (IHC) was performed using an anti-mCherry antigen on sections from the indicated tissues on the transgenic RM (top) and a wild-type control (bottom). **B)** The graph displays dPCR quantification of mCherry+ cells in the indicated tissues (left) or sorted cell populations (right). The percentage of mCherry gene-positive cells was calculated as the ratio of mCherry (single-copy gene) relative to the control RPP30 gene (diploid gene).

Figure 4: Increase in mCherry RNA expression after brief cell culture of primary cells. **A)** Images show representative brightfield (left), mCherry fluorescence (middle), and merged field (right) for primary hepatocytes

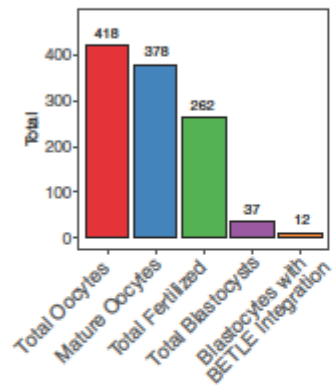
after culture for one day (top) and seven days (bottom). **B)** The graph displays dPCR quantification of mCherry expression at the indicated timepoints. Expression was calculated as the ratio of mCherry cDNA relative to the cDNA from the control RPP30 gene, which was normalized against the ratio in non-cultured cells.

Figure 5: ATAC-seq demonstrates epigenetic remodeling of BETLE after cell culture. ATAC-seq was performed in triplicate using isolated nuclei from primary skin fibroblasts before (P0) and after passage in cell culture (P4). The cells were negative for mCherry fluorescence at P0 and acquired fluorescence by P4. **A)** The graph summarizes peak accessibility in the genomic region surrounding the BETLE integration on chromosome 5. Data from P0 is shown on top, with P4 shown below. No significant changes were identified in the region surrounding the integration site. **B)** Identical data as **(A)**, showing only the BETLE cassette. The BETLE region has adopted a more accessible chromatin structure after cell culture.

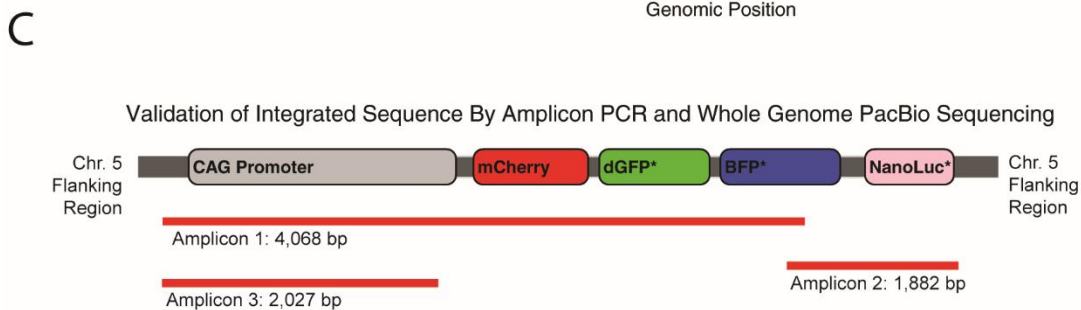
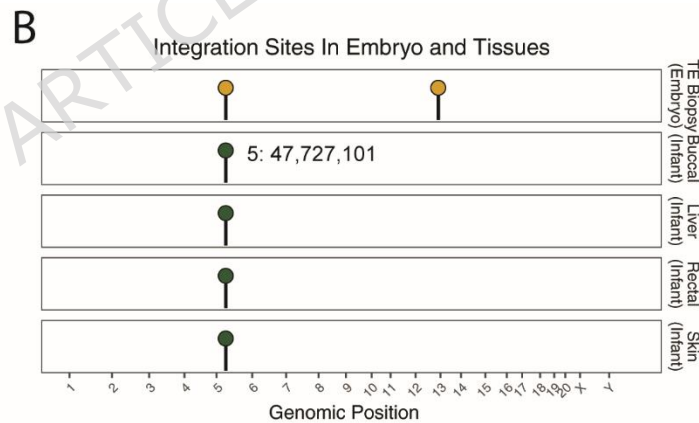
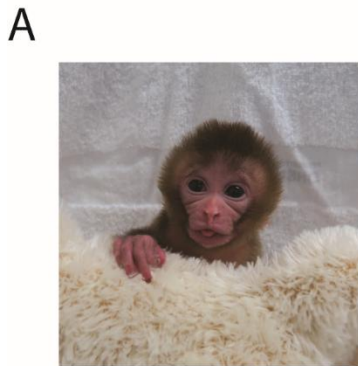
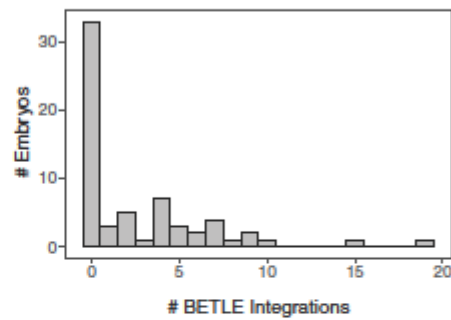
Figure S1: Increase in mCherry RNA expression after brief cell culture of primary fibroblasts. Images show representative mCherry fluorescence in primary skin fibroblasts after 65 days in culture. Cells from the BETLE-encoding transgenic RM are in the top-left, with three wildtype RMs shown in the other panels.

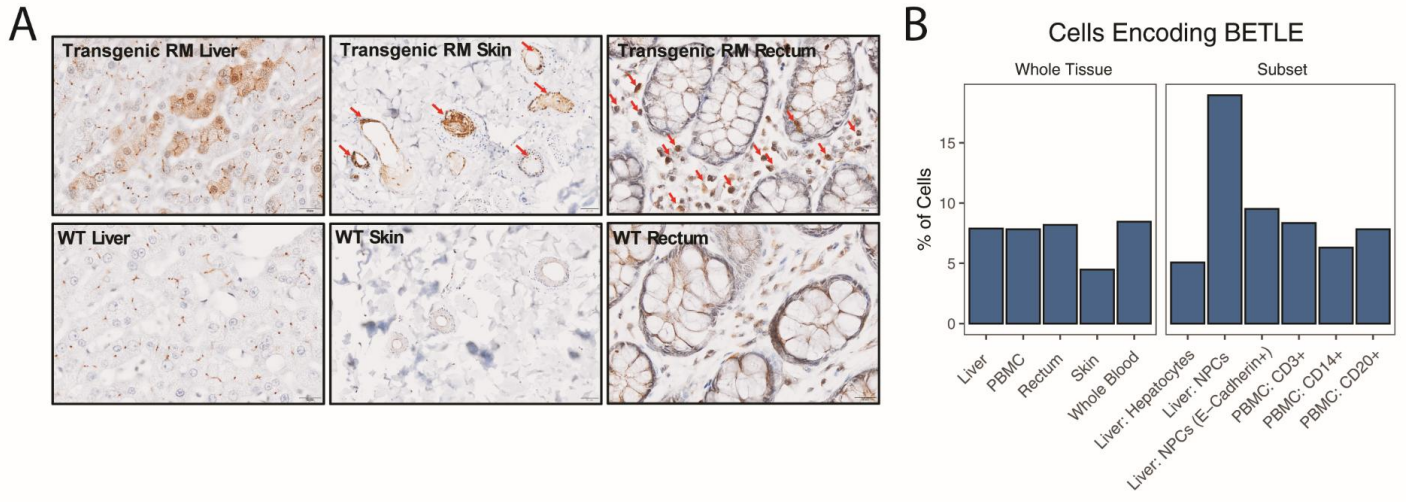


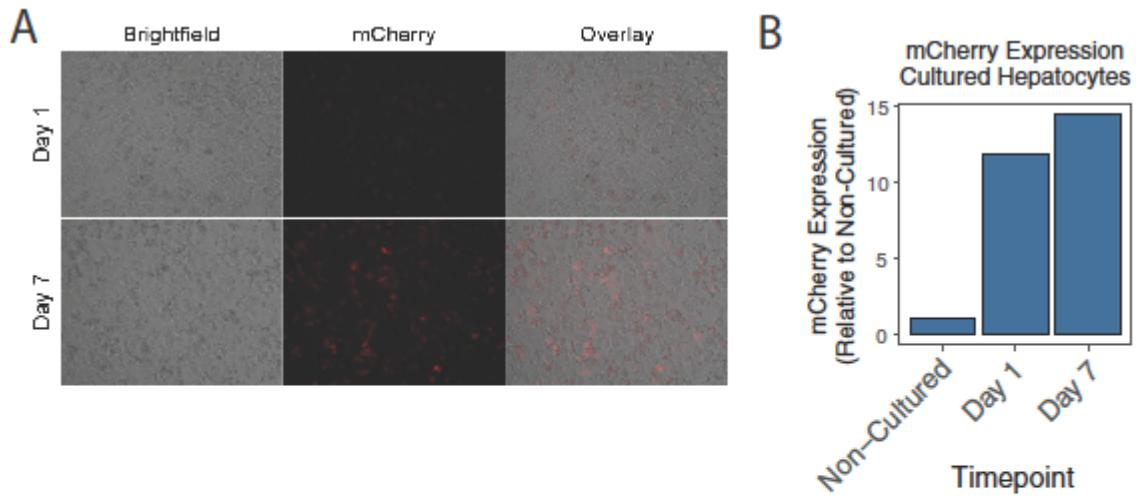
B Embryo Production and Editing Efficiency



C BETLE Integrations/Embryo







ARTICLE IN PRESS